HHS Public Access

Author manuscript

ACS Nano. Author manuscript; available in PMC 2021 December 01.

Published in final edited form as:

ACS Nano. 2017 June 27; 11(6): 5417–5429. doi:10.1021/acsnano.6b08152.

Dual Targeting Nanoparticle Stimulates the Immune System To Inhibit Tumor Growth

Alyssa K. Kosmides[†,‡,§], **John-William Sidhom**[†,§], **Andrew Fraser**[†,§], **Catherine A. Bessell**[§,‖], **Jonathan P. Schneck**[*,‡,§,‖]

[†]Department of Biomedical Engineering, Johns Hopkins University School of Medicine, Baltimore, Maryland 21231, United States

[‡]Institute for Nanobiotechnology, Johns Hopkins University School of Medicine, Baltimore, Maryland 21231, United States

[§]Institute for Cell Engineering, Johns Hopkins University School of Medicine, Baltimore, Maryland 21231, United States

[‖]Department of Pathology, Johns Hopkins University School of Medicine, Baltimore, Maryland 21231, United States

Abstract

We describe the development of a nanoparticle platform that overcomes the immunosuppressive tumor microenvironment. These nanoparticles are coated with two different antibodies that simultaneously block the inhibitory checkpoint PD-L1 signal and stimulate T cells *via* the 4-1BB co-stimulatory pathway. These “immunoswitch” particles significantly delay tumor growth and extend survival in multiple *in vivo* models of murine melanoma and colon cancer in comparison to the use of soluble antibodies or nanoparticles separately conjugated with the inhibitory and stimulating antibodies. Immunoswitch particles enhance effector-target cell conjugation and bypass the requirement for *a priori* knowledge of tumor antigens. The use of the immunoswitch nanoparticles resulted in an increased density, specificity, and *in vivo* functionality of tumor-infiltrating CD8+ T cells. Changes in the T cell receptor repertoire against a single tumor antigen indicate immunoswitch particles expand an effective set of T cell clones. Our data show the potential of a signal-switching approach to cancer immunotherapy that simultaneously targets two stages of the cancer immunity cycle resulting in robust antitumor activity.

Graphical Abstract

[*]**Corresponding Author:** jschnec1@jhmi.edu.

Supporting Information

The Supporting Information is available free of charge on the ACS Publications website at DOI: 10.1021/acsnano.6b08152.

Nanoparticle characterization, *in vitro* model characterization, effector-target cell conjugation studies, *in vivo* T cell analyses (PDF)

The authors declare no competing financial interest.

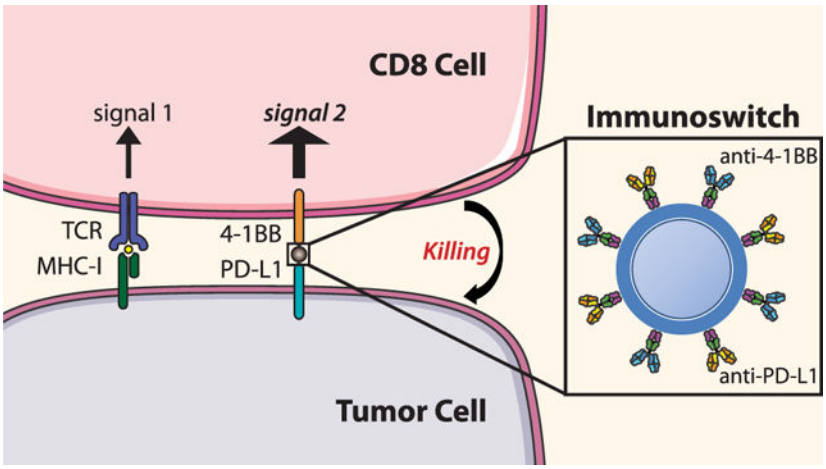

Keywords

cancer immunotherapy; nanoparticle; combination therapy; CD8+ T cell; T cell receptor repertoire; melanoma; colon cancer

Cancer provokes an immune response to tumor-associated antigens. This can initiate the activation of tumor-specific T cells and result in tumor cell death in a process known as the cancer-immunity cycle.[1] Cancer thrives when there is a blockade in this cycle that allows cancer escape, and current immunotherapeutics aim to take down these barriers.[2]

Many emerging immunotherapies target activation of a tumor-specific T cell response.[3–7] T cell activation can be initiated by ligating two necessary signals—the T cell receptor with its cognate peptide-MHC, termed signal 1, and a co-stimulatory molecule, termed signal 2—using cellular or nanoparticle-based platforms. Different molecules can serve as co-stimulatory signals to T cells[8] such as B7-1/B7-2 or 4-1BBL which bind to CD28 and 4-1BB on the T cell, respectively. Signaling through 4-1BB in particular has gained interest in recent years for its ability to induce a more effective antitumor immune response than CD28 alone. Ligation of 4-1BB on T cells has been demonstrated to enhance cytotoxicity, prevent activation-induced cell death, and increase expansion and cytokine secretion preferentially in cytotoxic CD8+ T cells.[9–11] Despite the ability of 4-1BB activation to initiate and maintain more effective tumor-targeting CD8+ T cells, the tumor microenvironment often upregulates immunosuppressive surface antigens and cytokines that diminish their cytotoxic effects.[12–17] Programmed death ligand 1 (PD-L1) is one such cell surface antigen, a checkpoint molecule upregulated on many cancers including melanoma, ovarian cancer, renal cell cancer, and non-small cell lung cancer.[18] Since a large proportion of tumor-infiltrating lymphocytes express PD-L1's receptor, programmed death 1 (PD-1),[6] expression of PD-L1 suppresses tumor-infiltrating lymphocyte effector functions.[19,20]

Monoclonal antibodies (mAb) that block checkpoint molecules such as PD-1, PD-L1, and CTLA-4 delay tumor growth in murine melanoma models,[19,21] and anti-PD-1 and anti-CTLA-4 mAb have been approved by the FDA with overall patient response rates of up to approximately 30%.[22–25] While expression of PD-L1 within the tumor microenvironment

correlates with outcome, its overall expression cannot predict response, indicating that there are other mechanisms at play.[26] Complete response rates in these patients have been as low as 5%[27] and demonstrates the need for additional development.

Recent studies have shown that checkpoint blockade efficacy can be further improved through combination with immunotherapies targeting diverse pathways. For example, a clinical trial combining PD-1 and CTLA-4 blockade nearly doubled survival time compared to anti-PD-1 mAb alone.[28] Additional studies in mice have shown similar results, with superior tumor control in mice treated with PD-1 antagonists in combination with CTLA-4 checkpoint blockade and 4-1BB co-stimulation.[29,30] However, these nonspecific approaches require high concentrations of antibody, as high as 100–200 μg/dose in murine models, and a majority of patients experience significant off-target side effects, especially when treated with a combination of antibodies.[28] Improvements in combinatorial immunotherapeutics are thus imperative to enable their use at safe and effective levels.

Here, we describe our development of a nanoparticle platform for combinatorial immunotherapeutics. These nanoparticles, termed immunoswitch particles, switch off the immunosuppressive PD-L1 pathway on tumor cells while simultaneously switching on the co-stimulatory 4-1BB pathway on CD8+ T cells. By physically constraining the antibodies on a nanoparticle platform, immunoswitch particles result in synergy between the two immunotherapies and are thus effective at low doses. *In vivo* we found that immunoswitch treatment had significant antitumor activity in both murine melanoma and colon cancer models and that the antitumor activity was seen with or without a model foreign antigen. The particles increase tumor-specific CD8+ T cell activation as compared to soluble antibody and do not require *a priori* selection of a cognate signal 1, allowing for activation of a robust polyclonal response. We show that immunoswitch particles mediate not only an increase in the number and specificity of tumor-specific CD8+ T cells but also a change in the endogenous T cell receptor repertoire. This conserved change demonstrates that therapy recruits an altered set of T cell receptors for more effective recognition even when recognizing a defined tumor antigen. Immunoswitch particles represent a signal-switching approach to T cell-mediated cancer immunotherapy that simultaneously targets two stages of the cancer immunity cycle.

RESULTS AND DISCUSSION

Immunoswitch Particles Activate PD-1^{hi} CD8+ T Cells *in Vitro*.

Immunoswitch particles link checkpoint blockade with T cell co-stimulation on a single nanoparticle platform. The particles are synthesized by conjugating 80 nm iron-dextran nanoparticles with a 1:1 molar ratio (Supplementary Figure 1A,B) of agonistic antibodies against 4-1BB (a co-stimulatory receptor found on the effector T cells) and antagonistic antibodies against PD-L1 (found on the cancer cells) (Figure 1A, inset). The hypothesized mechanism of action of the immunoswitch particles is shown in a schematic in Figure 1A – the particles target tumor cells expressing PD-L1 and simultaneously block access to PD-1 on T cells. Their co-stimulatory antibody binds to 4-1BB on CD8+ T cells, targeting them to the tumor cells and thus switching a negative signal into a co-stimulatory signal. The

clonotypic T cell receptor on the CD8+ T cell receives cognate signal 1 stimulation from the tumor cell itself.

Immunoswitch particle activity was analyzed *in vitro* using a model of repetitive antigen stimulation known to mimic the tumor microenvironment.[31] 2C T cell receptor transgenic CD8+ T cells, specific for the SIY peptide presented in the context of the H-2 Kb MHC, were repetitively stimulated with anti-CD3/anti-CD28 expander beads. Murine melanoma cells—either noncognate B16-F10 cells or cognate B16-SIY cells, a transfected tumor cell line derived from B16-F10 that expresses the cognate Kb-SIY antigen—were treated with 20 ng/mL IFN-γ. These treatments resulted in upregulation of PD-1 and 4-1BB expression on the CD8+ T cells (Supplementary Figure 2A) and upregulation of PD-L1, but not PD-L2, on the murine melanoma cells (Supplementary Figure 2B,C). Treatment with either soluble anti-4-1BB or anti-PD-L1 mAb increased CD8+ T cell activation in a dose-dependent fashion, demonstrating the ability to study immunoswitch nanoparticle activity in this model (Supplementary Figure 3A,B).

PD-1^{hi} CD8+ T cells and PD-L1^{hi} B16-SIY cells were co-incubated with immunoswitch particles, and T cell stimulation was measured by IFN-γ secretion. Compared to cultures treated with isotype particles, there was maximally over a 6-fold increase in IFN-γ secretion by immunoswitch particle-treated cultures (Figure 1B). As expected, cultures treated with soluble anti-4-1BB and anti-PD-L1 also increased IFN-γ secretion, although only a 2- to 3-fold increase over isotype antibody controls. These data show that the antibodies maintain their functionality even when constrained on nanoparticles and in fact potentially have increased T cell stimulatory activity.

To investigate the requirement for both antibodies on the surface of the nanoparticle, we compared CD8+ T cell activation in response to co-incubation with immunoswitch particles *versus* anti-4-1BB mAb only or anti-PD-L1 mAb only particles. The greatest IFN-γ secretion, maximally 173 ± 3 ng, was measured in immunoswitch particle treated cultures (Figure 1C). In contrast, only 141 ± 18 ng and 107 ± 8 ng of IFN-γ was produced by cultures treated with anti-4-1BB and anti-PD-L1 only particles, respectively.

Immunoswitch Particles Enhance T Cell-Tumor Cell Conjugation.

To understand the mechanism of immunoswitch particle activity, we studied their cellular interactions. We sought to investigate both their ability to mediate CD8+ T cell-tumor cell conjugation as well as requirements for cognate peptide-MHC stimulation.

We investigated the requirement for peptide-MHC recognition by comparing 2C CD8+ T cell activation when co-incubated with immunoswitch particles and cognate B16-SIY or noncognate B16-F10 tumor cells. In the presence of B16-SIY cells, immunoswitch particles resulted in robust IFN-γ secretion (Figure 1D). There was no IFN-γ secretion in response to immunoswitch particles when 2C CD8+ T cells were stimulated with B16-F10 tumor cells lacking the cognate antigen. We further investigated the signal 1 dependence of immunoswitch activation by measuring cytotoxicity of cognate tumor cells *in vitro*. 2C CD8+ T cells were co-incubated with cognate B16-SIY cells, immunoswitch particles, and an anti-Kb mAb to block the signal 1 peptide-MHC interaction. At a 1:1 effector-target

cell ratio, immunoswitch particles resulted in 22.8% specific lysis of B16-SIY cells (Figure 1E). This was reduced to only 2.16% when an anti-Kb mAb was included during the co-incubation. Immunoswitch particle stimulation and cytotoxicity is dependent on the CD8+ T cell receiving a cognate signal 1 from the tumor cell itself.

In addition to requiring a cognate tumor cell for CD8+ T cell activation, we also investigated the hypothesis that immunoswitch particles increase effector-target cell conjugation. 2C CD8+ T cells and B16-F10 melanoma cells were labeled with a red and green membrane dye, respectively. Noncognate B16-F10 cells were chosen to eliminate conjugate formation mediated by the T cell receptor-peptide-MHC interaction.

Labeled 2C CD8+ T cells and B16-F10 cells were co-incubated in the presence of immunoswitch or isotype particles. After 1 h, cells were fixed and conjugate formation was measured by confocal microscopy or flow cytometry. Confocal microscopy showed an increase in effector-target cell conjugation mediated by immunoswitch particles (Figure 1F, Supplementary Figure 4A). At a 420 ng/mL total antibody dose, immunoswitch particles resulted in significantly higher conjugate formation than isotype particles, nearing 30% of CD8+ T cells conjugated to tumor targets. Isotype particles resulted in minimal conjugate formation, indicating that PD-1/PD-L1 expression plays little to no role in effector-target cell conjugation in this system. The results of confocal microscopy were validated by a flow cytometry-based conjugation assay. 420 ng/mL of immunoswitch particles resulted in significantly greater effector-target cell conjugation as compared to isotype (Supplementary Figure 4B). These results indicate that immunoswitch particles increase conjugation by physically linking effector and target cells in an antigen-independent fashion.

Immunoswitch Particles Inhibit Tumor Growth *in Vivo*.

We investigated the efficacy of immunoswitch nanoparticle treatment in several *in vivo* models. Our first model, based on our *in vitro* system, was an adoptive transfer of the repetitively stimulated PD-1^{hi} tumor-specific 2C CD8+ T cells into mice with pre-established B16-SIY melanoma tumors, followed at intervals by immunoswitch particles. Adoptively transferred cells were used as a model of exhausted tumor-specific cells that would likely be present in a patient's tumor microenvironment prior to treatment.

C57BL/6 mice were injected with 1×10^6 B16-SIY tumor cells on day 0, and 5×10^5 PD-1^{hi} 2C CD8+ T cells were adoptively transferred on day 8 (Figure 2A, schematic). T cell recipients were treated with immunoswitch particles on days 8, 11, and 15 or with various controls: (1) PD-1^{hi} 2C CD8+ T cells alone, (2) PD-1^{hi} 2C CD8+ T cells + isotype-conjugated particles, or (3) PD-1^{hi} 2C CD8+ T cells + soluble anti-4-1BB mAb + soluble anti-PD-L1 mAb. All treatment groups received a total of 1.3 μg of antibody per mouse per treatment intratumorally, approximately 10–100-fold less than the amount typically used for systemic treatment.[29,30,32]

Immunoswitch treatment significantly delayed tumor growth compared to all other groups ($p < 0.001$). Adoptive cell transfer alone, isotype particles, and soluble antibody did not result in significant slowing of tumor growth compared to no treatment (Figure 2B). This indicates that the particles themselves do not have any effect due to the intratumoral injection and

that conjugating the antibodies to a rigid nanoparticle is necessary for their antitumor activity. Additionally, immunoswitch particles were the only treatment to significantly extend survival (Figure 2C); mice died later or not at all by day 31. Soluble antibody also extended survival in a small number of mice, although this change was not statistically significant.

In our second *in vivo* model, we analyzed immunoswitch particle activity *in vivo* in the absence of adoptively transferred T cells in the pre-established B16-SIY model (Figure 3A, schematic). Controls included no treatment or animals co-injected with a mixture of single-coated anti-4-1BB only and anti-PD-L1 only particles. This second control was included to investigate the importance of effector-target cell conjugation seen *in vitro* on *in vivo* activity. If immobilizing the antibodies on a rigid nanoparticle platform is sufficient for activity, then we would expect both immunoswitch particles and separately conjugated nanoparticles to perform equivalently.

Only immunoswitch treated animals had delayed tumor growth and extended survival compared to all other groups (Figure 3B,C). By day 18, nontreated and separate particle-treated mice had an average tumor size of approximately 176 mm^2, whereas immunoswitch particle-treated mice had an average tumor size of nearly half, approximately 95 mm^2. This indicates that immunoswitch particles stimulate the polyclonal endogenous repertoire of CD8+ T cells and that both antibodies must be presented by the same nanoparticle for *in vivo* activity.

Immunoswitch Particles Activate Endogenous T Cells.

To mechanistically study how immunoswitch particles activate an immune response, we analyzed tumor-infiltrating lymphocytes and tumor-draining lymph nodes of immunoswitch treated animals. C57BL/6 mice were injected with B16-SIY tumor cells on day 0. Immunoswitch particles were administered days 8 and 11, and tumors and tumor-draining lymph nodes were harvested and analyzed on day 14.

As expected, immunoswitch treated mice had significantly smaller tumors (Figure 3D). The density of CD8+ T cells within the tumor-infiltrating lymphocyte compartment more than doubled in the immunoswitch treated group compared to no treatment (Figure 3D), while CD4+ T cell density remained unchanged (Supplementary Figure 5). The impact of immunoswitch treatment on antigen-specific T cells was analyzed by determining the Kb-SIY-specific CD8+ T cell response to the B16-SIY tumors. There were approximately double the percentage of Kb-SIY positive CD8+ T cells within the tumor-draining lymph node of immunoswitch treated animals compared to nontreated animals: 0.49 ± 0.2% and 0.22 ± 0.1%, respectively (Figure 3E,F), while no difference in Kb-SIY positive CD8+ T cells were seen within the spleen, peripheral blood (Supplementary Figure 6), or tumor-infiltrating lymphocytes (Supplementary Figure 7a).

Since immunoswitch treated mice have significantly delayed tumor growth, we hypothesized that treatment may increase the functionality of tumor-infiltrating lymphocytes. To study the functionality of Kb-SIY+ CD8+ tumor-infiltrating lymphocytes following immunoswitch treatment, mice were treated, and tumor-infiltrating lymphocytes harvested on day 14 as

above. Tumor-infiltrating lymphocytes were restimulated *in vitro* with SIY pulsed RMA-S cells, and cytokine and CD107 production analyzed.

Immunoswitch treated animals had more than double the percentage of CD8+ tumor-infiltrating lymphocytes expressing CD107, a degranulation marker and indicator of the ability of T cells to lyse target tumor cells (Figure 4A). CD8+ tumor-infiltrating lymphocytes also produced more IFN-γ compared to tumor-infiltrating lymphocytes from nontreated mice (Figure 4B,C). This was seen by both an increase in the percent of IFN-γ+ cells (Figure 4B) and a 38% increase in the mean fluorescence intensity of IFN-γ+ cells, indicating greater per-cell production (Figure 4C). Together, these data indicate that immunoswitch particles stimulate an antitumor CD8+ T cell response by increasing their density, local tumor specificity, and *in vivo* functionality, consistent with findings that anti-4-1BB mAb primarily targets CD8+ T cells.[10]

Immunoswitch Particles Alter the T Cell Receptor Repertoire.

To gain a deeper understanding of the mechanism of action of immunoswitch particles, we analyzed the T cell receptor repertoire of the tumor-infiltrating CD8+ T cells. As described above, tumors were harvested on day 14, tumor-infiltrating CD8+ T cells were sorted, and T cell receptors sequenced to determine amino acid sequence of the CDR3 region of the T cell receptor beta chains (T cell receptor V-beta). V-beta usage by the tumor-infiltrating lymphocytes of each treatment group was compared to usage in a naïve C57BL/6 mouse and to a Kb-SIY-specific response obtained by using a previously established CD8+ T cell activation protocol[33] to expand Kb-SIY-specific cells from splenocytes of naïve C57BL/6 mice. After a 7 day stimulation, Kb-SIY+ CD8+ T cells were sorted and sequenced (Supplementary Figure 7B). As seen previously by Kb-SIY peptide-MHC staining of the tumor-infiltrating lymphocytes, the primary response of both immunoswitch-treated and tumor-bearing nontreated mice was dominated by V-beta 13, which is characteristic of a Kb-SIY response (Figure 5A).

Despite the similarity in V-beta usage, the T cell receptor repertoire of these cells was significantly altered by immunoswitch treatment. T cell receptor clones, defined by the amino acid sequence of the CDR3 region, present in the tumor-infiltrating lymphocytes of immunoswitch treated mice appear at significantly lower levels in nontreated mice (Figure 5B). Similarly, T cell receptor clones present in nontreated mice are present at significantly lower levels than in immunoswitch treated mice (Figure 5B). This indicates that although a majority of the response both in the presence and absence of treatment is specific for the tumor-expressed Kb-SIY model antigen, the clones making up this response are changed by immunoswitch therapy.

Next, we investigated the conservation of this changed CD8+ T cell response after immunoswitch treatment. The clones that make up the majority of the response between pairs of immunoswitch-treated mice overlap by 44.1 ± 4.3% (Figure 5C). This contrasts with only 6.43 ± 6.92% of an overlapping response between pairs of nontreated mice. Thus, immunoswitch particle treatment selects for a highly conserved antitumor response. This indicates that treatment delays tumor growth by inducing expansion of a specific population of antitumor CD8+ T cells with an altered T cell receptor sequence signature.

Immunoswitch Particles Prolong Retention at Treatment Site.

In addition to altering the immune response, nanoparticles are larger than soluble antibody and thus have a different biodistribution.[34,35] Therefore, we sought to characterize the pharmacokinetics of immunoswitch particle treatment. We hypothesized that immunoswitch particles would diffuse from the injection site more slowly than soluble antibodies, resulting in a higher average concentration over time.

Immunoswitch particles or an equivalent amount of soluble antibody were labeled with an infrared (IR) dye and injected subcutaneously into nude mice. Mice were imaged using a full body IR imager after 3, 24, 48, and 72 h to quantify biodistribution. Soluble antibody was cleared from the injection site significantly more rapidly than immunoswitch particles (Figure 6A,B). By 24 h, approximately 72% of immunoswitch particles, but only 26% of soluble antibody, remained at the injection site. Within 72 h, this decreased to 60% of immunoswitch particles and 8% of soluble antibody. A fit of the data to one-phase decay equations showed a half-life of 15.2 h for soluble antibody compared to 84.5 h for immunoswitch particles.

Similarly sized nanoparticles have been shown to drain to the proximal tumor-draining lymph node following intratumoral injection but not to more distal sites, minimizing systemic toxicity.[35] We therefore examined the organ biodistribution of immunoswitch particles following intratumoral injection. C57BL/6 mice were injected with IR-labeled immunoswitch particles 8 days after B16-SIY tumor inoculation. 48 h after treatment, the tumor, tumor-draining lymph node, contralateral lymph node, and spleen were dissected and imaged by an IR imager. Immunoswitch particles were found in the tumor and tumor-draining lymph node (Figure 6C), consistent with our finding that tumor-specific CD8+ T cells are present at higher levels in the tumor-draining lymph node of immunoswitch treated mice. There were little to no detectable levels of immunoswitch particles in the contralateral lymph node or spleen. Prolonged retention of the immunoswitch particles at the tumor site and tumor-draining lymph node may contribute to their increased efficacy over soluble antibody. This sequestration of immunostimulatory ligands at the tumor site is consistent with the findings of others in the development of nanocarriers for tumor microenvironment immunomodulation.[34,35]

Immunoswitch Particles Reverse Tumor Growth in Multiple Cancer Models.

We sought to investigate the broader applicability of immunoswitch particles by assessing treatment in additional tumor models, colon cancer and B16-F10, and through a different injection route, IV administration. We first studied their efficacy in MC38-OVA, a murine colon cancer expressing a model foreign antigen, OVA. C57BL/6 mice were injected subcutaneously with MC38-OVA tumors on day 0. Mice were treated with immunoswitch or isotype particles intratumorally on days 8, 11, 15, and 18, and tumors were measured.

Immunoswitch treated mice had significantly delayed tumor growth, averaging 19 mm^2 on day 36, as compared to 158 mm^2 for nontreated mice and 126 mm^2 for isotype particle treated mice (Figure 7A). As compared with 10% of nontreated mice (Figure 7B), 70% of immunoswitch-treated mice survived past day 55. These effects were even more

pronounced than those seen in the B16-SIY model. In 5 of 10 mice, immunoswitch particle treatment led to complete regression of palpable MC38-OVA tumors. The MC38-OVA cell line also expresses different peptide-MHC from B16-SIY, demonstrating the robustness of immunoswitch treatment in the absence of adoptively transferred cells.

The tumor models B16-SIY and MC38-OVA both express strong model foreign antigens. Thus, we next sought to investigate the efficacy of immunoswitch particle therapy in a less immunogenic tumor model, B16-F10, which is identical to B16-SIY except that it lacks expression of the Kb-SIY model foreign antigen, to demonstrate broader therapeutic relevance.

C57BL/6 mice were injected subcutaneously with B16-F10 tumors on day 0. Mice were treated with immunoswitch particles intratumorally on days 8, 11, and 15, and tumors were measured. Immunoswitch particle therapy resulted in significantly delayed tumor growth compared to nontreated mice (Figure 7C). By day 15, the tumor size was nearly halved by immunoswitch treatment; tumors averaged 112 mm^2 for immunoswitch-treated mice compared to 205 mm^2 for nontreated mice. Immunoswitch particle treatment also resulted in significantly extended survival compared to no treatment. These data demonstrate the broader applicability of immunoswitch particle therapy to less immunogenic tumor models.

Immunoswitch Particles Delay Tumor Growth When Injected Intravenously.

Finally, we further investigated the route of administration by studying the effect on tumor growth when injected intravenously. C57BL/6 mice were injected subcutaneously with B16-SIY tumors and were treated with immunoswitch particles intravenously on days 4, 8, 11, and 15. Mice treated with immunoswitch particles intravenously were given one additional early dose on day 4, a standard time point used for checkpoint inhibition studies in the B16-SIY model.[29] Intravenous treatment resulted in similar antitumor efficacy to our standard intratumoral treatment (Figure 7D). In contrast, similar doses of IV administered soluble antibody had no effect on tumor growth, as was seen with intratumoral injection of soluble antibodies.

CONCLUSION

Combinatorial immunotherapy for cancer treatment has resulted in promising success in clinical trials. However, the use of nonspecific immunomodulators, such as checkpoint blockade, requires high doses of the drugs and results in significant off-target side effects, especially when multiple drugs are used in combination.[28] Thus, there is incentive to develop more effective and less toxic treatments. Sequestering immunotherapeutics on a rigid nanoparticle platform alters their biodistribution and may reduce off-target toxicities. In this way, Kwong *et al.* have laid the groundwork in the development of nanoparticles to deliver and present immunostimulatory ligands, such as anti-4-1BB or anti-CD40, to CD8+ T cells and other immune cells.[34,35] However, their nanoparticles were not designed to target two different cell types in the tumor microenvironment. Immunoswitch nanoparticles do this, linking immunomodulators differentially expressed on CD8+ T cells and target cells within the tumor, and have significant antitumor activity *in vivo*.

We have created an immunoswitch nanoparticle that blocks the immunosuppressive PD-L1 pathway while switching on the 4-1BB co-stimulatory pathway of tumor-targeting CD8+ T cells on a single injectable platform. These particles utilize spatial constraints to enhance the efficacy of two developing immunotherapies. Immunoswitch particles inhibited tumor growth more effectively than equivalent amounts of soluble anti-PD-L1 and anti-4-1BB mAb. While tethering the antibodies to a rigid particle platform increases avidity for their ligand and may play a role in their efficacy, we identified at least two additional mechanisms that explain immunoswitch-based T cell activation and antitumor activity.

Combining both anti-PD-L1 and anti-4-1BB mAb on a single platform physically links the effector and target cells. This was directly shown *in vitro* by confocal microscopy and flow cytometry. The importance of the physical linkage of both antibodies to a single nanoparticle was also seen *in vivo* despite the complexity of the tumor microenvironment; co-injected separately conjugated particles, bearing either anti-PD-L1 or anti-4-1BB mAb, were ineffective. Additionally, we showed that immunoswitch particles diffuse from the injection site more slowly than their soluble counterpart. This implies a higher local concentration of the bioactive particles integrated over time and consequently a decreased concentration at off-target sites. Although soluble antibody and separately conjugated particles had some *in vitro* activity, stimulating IFN-γ secretion, they had no *in vivo* effect. In contrast, immunoswitch treatment had significant antitumor activity *in vivo*. Thus, *in vitro* IFN-γ secretion may not fully explain *in vivo* activity where other factors, such as biodistribution and shaping of the endogenous T cell receptor repertoire, may play a larger role.

While the immunoswitch particles led to antigen-independent effector-target cell conjugation, target cell recognition and IFN-γ effector cytokine secretion were signal 1 dependent. This was demonstrated *in vitro* when transgenic 2C CD8+ T cells were not stimulated by immunoswitch particles in the presence of noncognate target cells. However, *a priori* knowledge of the tumor antigen is not necessary since signal 1 is derived from the tumor cell itself. Thus, immunoswitch particles can activate a diverse polyclonal T cell response *in vivo* and reduce the chance of antigenic escape.[36]

Murine melanoma tumor control mediated by immunoswitch particles was observed even in the absence of adoptively transferred tumor-specific CD8+ T cells and when administered systemically by intravenous treatment. We showed that immunoswitch particles exert their effect by increasing the density, specificity, and functionality of endogenous tumor-specific CD8+ T cells. Tumor-infiltrating lymphocytes of immunoswitch treated mice increased IFN-γ production and CD107 expression. In addition, more IFN-γ was made on a per cell basis as seen by an increase in IFN-γ mean fluorescence intensity (MFI) after immunoswitch treatment. There was no difference in tumor-specific CD8+ T cell levels in the spleen or in circulation, indicating that immune activation is concentrated to the tumor site and thus may limit off-target immune-mediated toxicities, as supported by the particle biodistribution. Additionally, this approach may be generally applicable, as tumor control was also evident in an MC38-OVA colon cancer model and in a less immunogenic B16-F10 melanoma cancer model lacking a model foreign antigen. Immunoswitch particles thus activate the endogenous T cell repertoire against a variety of tumor antigens.

Finally, sequencing analysis of the tumor-infiltrating lymphocytes revealed that the immunoswitch-mediated anti-tumor response is mediated by a change in the T cell receptor repertoire. Immunoswitch particle treatment expands a different set of CD8+ T cell receptor clones not present at high levels in nontreated mice. This altered T cell receptor repertoire is highly conserved, indicating that treatment enables the immune system to find the "correct" antitumor immune response without switching recognition to a different antigen. While many existing therapies induce alterations in the breadth and depth of the T cell response,[37,38] we show that immunoswitch particles change the clonal composition of the response against a defined tumor antigen.

Immunoswitch particles are an immunotherapy that utilizes a single, nanoparticle-based injectable therapeutic. By combining multiple targeting moieties on the surface of a single particle, this represents a genre of nanoparticle-based approaches for cancer immunotherapy. The increased effectiveness of immunoswitch particles over soluble antibody can allow for reduced cost and complexity of a multifaceted therapeutic. The nanoparticle platform also allows for further modifications to optimize biodistribution or deliver signals locally. For example, nanoparticle size or shape can be engineered to reduce clearance or target-specific cell types,[39,40] and the core can be designed to release an immune-stimulant such as IL-2.[41] Additionally, we have shown proof of concept of a "signal-switching" approach that links two signaling pathways. This can be extended to other parts of the cancer-immunity cycle, including other inhibitory and/or co-stimulatory pathways, such as Lag-3, CTLA-4, or CD28, in addition to pathways relevant in autoimmunity and other disease states. Thus, immunoswitch particles are a nanoparticle-based combination therapy and build a framework for further mechanistic and translational studies.

METHODS

Mice.

2C T cell receptor transgenic mice were maintained as heterozygotes by breeding on a C57BL/6 background. C57BL/6 and Nu/J mice were purchased from Jackson Laboratories (Bar Harbor, ME, USA). All mice used were 6–8 weeks of age and were maintained according to Johns Hopkins University's Institutional Review Board.

Cell lines.

B16-SIY was a gift from Thomas Gajewski (The University of Chicago, IL, USA). B16-F10 and MC38-OVA were a gift from Charles Drake (Johns Hopkins University, MD, USA). RMA-S cells were a gift from Michael Edidin (Johns Hopkins University, MD, USA). Tumor cell lines have been authenticated by cognate T cell cytotoxicity.

Reagents.

Anti-PD-L1 monoclonal antibody clone 10F.9G2, anti-4-1BB clone 3H3, anti-CD3 clone 145.2C11, anti-CD28 clone 37.51, and their respective isotype controls were purchased from BioXCell (West Lebanon, NH, USA). Fluorescently labeled monoclonal antibodies were purchased from BioLegend (San Diego, CA, USA). SIY peptide was purchased from GenScript (Piscataway, NJ, USA).

Immunoswitch Particle Synthesis and Characterization.

Antibiotin-coated iron-dextran 50–100 nm particles were purchased from Miltenyi (Miltenyi Biotec, Auburn, CA, USA). Anti-PD-L1 antibody clone 10F.9G2, anti-4-1BB clone 3H3, and their respective isotype controls were biotinylated using EZ-Link sulfo-NHS-biotin (Thermo Fisher Scientific, Waltham, MA, USA) according to the manufacturer's protocol. Particles and a 2-fold molar excess of the biotinylated antibodies of interest were combined and allowed to conjugate for 24 h at 4 °C. Unbound antibody was removed by running the particles over an MS column (Miltenyi Biotec, Auburn, CA) and washing according to the manufacturer's protocol.

Particle size was determined by nanoparticle tracking analysis using a Nanosight LM10. To characterize particle conjugation, a standard curve relating absorbance to particle concentration was made using a Beckman Coulter AD340 plate reader and Nanosight LM10. Particles were then subsequently measured for absorbance to determine concentration, and all particles were brought to a concentration of 1.4×10^{12} particles/mL. The amount of specific antibody per particle was determined by staining the particles with fluorescently labeled secondary antibodies against the antibody of interest. Excess antibody was removed by running the particles over an MS column (Miltenyi Biotec, Auburn, CA, USA), and antibody concentration was measured by comparing particle fluorescence to a standard curve and correlating with the total bead concentration.

In Vitro CD8+ T Cell Activation Model.

On day −8, primary splenocytes were isolated from naïve 2C transgenic mouse spleens through cell straining. Cells were treated with 4 mL of ACK lysis buffer for 1 min to lyse red blood cells. CD8+ T cells were isolated by negative selection with the Miltenyi CD8a+ isolation kit IIa following the manufacturer's protocol (Miltenyi, Auburn, CA, USA). Micro anti-CD3/anti-CD28 expander beads were synthesized on 4.5 μm M-450 Epoxy Dynabeads (Life Technologies, Grand Island, NY, USA) at a 1:1 molar protein ratio, following manufacturer's protocol. 2C CD8+ T cells were mixed with micro expander beads at a 1:1 ratio and cultured in RPMI supplemented with L-glutamine, non-essential amino acids, vitamin solution, sodium pyruvate, β-mercaptoethanol, 10% FBS, ciproflaxin, and a cocktail of T cell growth factors. On day −4, additional T cell growth factors and expander beads were added at a 2:1 bead:cell ratio. On day −2, B16-SIY and B16-F10 cells were cultured in RPMI supplemented with L-glutamine, non-essential amino acids, vitamin solution, sodium pyruvate, β-mercaptoethanol, 10% FBS, ciproflaxin, and 20 ng/mL recombinant murine IFN-γ (R&D Systems, Minneapolis, MN, USA).

On day 0, B16-F10 and B16-SIY were harvested and washed three times to remove all IFN-γ, as confirmed by ELISA. 2C cells were also harvested and washed three times, and beads were removed with a magnet. Live CD8+ cells were isolated by density centrifugation using Ficoll-Paque PLUS (GE Healthcare Life Sciences, Pittsburgh, PA, USA). Surface marker expression on both cell types was measured using a BD FacsCalibur flow cytometer and analyzed in FlowJo (TreeStar). For IFN-γ release studies, 2C cells and B16-SIY or B16-F10 cells were mixed at a 1:1 effector target ratio in the presence of particles or soluble antibody. The cells were incubated for 18 h at 37°, then supernatants were collected.

IFN-γ was measured by ELISA using the ebioscience murine IFN-γ Ready-SET-Go! Kit (San Diego, CA, USA). For cytotoxicity assay, 2C cells and B16-SIY cells were mixed at a 1:1 effector target ratio in the presence of immunoswitch particles and 100 μg/mL anti-Kb (clone 20.8.4) or respective isotype mAb. After 4 h, supernatant was harvested, and cytotoxicity was measured using a CytoTox-Glo Cytotoxicity Assay (Promega, Madison, WI, USA) according to the manufacturer's protocol. Luminescence was read on a Tropix TR717 Microplate Luminometer.

B16 *in Vivo* Tumor Growth Experiments.

Immunoswitch and isotype particles were synthesized and characterized as described above. Amount of antibody on the particles was quantified, and a solution of equal concentration nonbiotinylated antibody was diluted in PBS. Particles and soluble antibody were put to a concentration of 13 μg/mL total antibody (6.3 μg/mL anti-PD-L1 and 6.3 μg/mL anti-4-1BB), and treated mice received 100 μL each.

C57BL/6 mice were injected with 1×10^6 B16-SIY or 3×10^5 B16-F10 cells subcutaneously on the right flank on day 0. For adoptive transfer experiments, CD8+ cells were harvested from naïve 2C splenocytes and stimulated with anti-CD3/anti-CD28 expander beads on days 0 and 4 as described above. On day 8, when all mice had a palpable tumor, beads were isolated from CD8+ cells, and live cells were isolated by density centrifugation using Ficoll-Paque PLUS (GE Healthcare Life Sciences, Pittsburgh, PA, USA). Five $\times 10^5$ 2C CD8+ cells were intravenously injected into all groups (except for the no treatment group). For all experiments, isotype particles, immunoswitch particles, or soluble antibody were injected intratumorally on days 8, 11, and 15. For intravenous studies, immunoswitch particles or soluble antibody were injected retro-orbitally on days 4, 8, 11, and 15. Beginning on day 4–8, tumors were measured every 2–3 days using digital calipers, and tumor size was computed by multiplying the longest dimension by the length of the perpendicular dimension. Mice were sacrificed when tumor area surpassed 200 mm^2.

B16-SIY Tumor-Infiltrating Lymphocyte Analysis.

Immunoswitch particles were synthesized and characterized as above. C57BL/6 (Jackson Laboratories, Bar Harbor, ME, USA) mice were injected with 1×10^6 B16-SIY cells subcutaneously on day 0. Immunoswitch particle treatment was administered intratumorally on days 8 and 11 (n = 5/group).

On day 14, tumors were measured, and peripheral blood, tumors, spleens, and tumor-draining lymph nodes were isolated. Spleens and tumor-draining lymph nodes were brought to a single cell suspension using a cell strainer, washed, and then resuspended in PBS. Tumors were coarsely sectioned using scissors and then brought to a single cell suspension using a cell strainer. Tumor-infiltrating lymphocytes were isolated by density centrifugation using Ficoll-Paque PLUS (GE Healthcare Life Sciences, Pittsburgh, PA, USA), then washed three times, and resuspended in PBS. Cell counts were taken using a hemocytometer.

For phenotypic analysis, isolated cells were stained with a fluorescently labeled with a live/dead stain (Thermo Fish Scientific, Waltham, MA, USA), CD8 antibody (BioLegend, San Diego, CA, USA), and biotinylated Kb-SIY dimer, followed by fluorescently labeled

streptavidin. Cells were run on a BD LSR II flow cytometer and analyzed using FlowJo (TreeStar). CD8 cell density was measured by multiplying the CD8 purity measured by flow cytometry by the total cell count and dividing by the tumor volume (longest dimension squared and multiplied by the perpendicular dimension).

For functional analysis, an equivalent number of tumor-infiltrating lymphocytes from individual mice (n = 3/group) were co-incubated with SIY pulsed RMA-S cells and anti-CD107 FITC. After 12 h, GolgiStop/GolgiPlug (BD Biosciences, San Jose, CA, USA) were added to solution. Six hours later, cells were stained for surface markers, then fixed and permeabilized with BD Cytofix/Cytoperm, and stained with fluorescently labeled antibodies against intracellular cytokines according to the manufacturer's protocol. Labeled cells were read on an LSR II and analyzed with FlowJo.

T Cell Receptor Sequencing Analysis.

In vivo tumor administration and treatment was identical to that in the B16-SIY Tumor-Infiltrating Lymphocyte Analysis section (n = 3/group). On day 14, tumor-infiltrating lymphocytes were isolated as above. Isolated cells were stained with a fluorescently labeled anti-CD8 mAb and live/dead stain (Thermo Fish Scientific; Waltham, MA) and CD8 antibody (BioLegend; San Diego, CA), and each sample was sorted based on live/CD8+ cells. CD8+ cell samples were sent to Adaptive Biotechnologies for deep sequencing of the T cell receptor beta chain.

To assess V-beta usage analysis compared to a Kb-SIY response, spleens were isolated and pooled from three nontumor bearing C57BL/6 mice. CD8+ T cells were isolated by negative selection as described above, and stimulated for 7 days with Kb-SIY/anti-CD28 nano-aAPC according to our previously published enrichment + expansion protocol.[33] On day 7, cells were fluorescently labeled with a live/dead stain, CD8 antibody, and Kb-SIY dimer, as described above. Cells were sorted for live/CD8+/Kb-SIY+ and sent to Adaptive Biotechnologies for sequencing.

To assess characteristics of T cell receptor sequence repertoire, tsv files from adaptive were downloaded from their online portal and converted to excel files, and the unproductive sequences were removed (only clones with amino acid CDR3 sequences were examined). All clones with the same amino acid sequence were combined, and their net frequency was calculated. In order to examine the presence of clones in either immunoswitch or nontreated cohorts, only sequences with a contribution above 0.5% were examined. To examine the conservation of the response between animals in both cohorts, the top 85% of the CD8+ T cells response was examined, and conservation of response was determined as the weighted average (by reads) an identical sequence makes up in the two samples being compared.

MC38-OVA *in Vivo* Tumor Model.

Immunoswitch particles and isotype particles were synthesized as described above. Amount of antibody on all particles was quantified by the methods described above, and particles were put at a concentration of 13 μg/mL total antibody. Treated mice received 100 μL particles/mouse.

C57BL/6 (Jackson Laboratories, Bar Harbor, ME, USA) mice were injected with 1×10^6 MC38-OVA cells subcutaneously on day 0, and cages were randomly assigned to one of three groups: (1) no treatment, (2) isotype particles, or (3) immunoswitch particles ($n = 6$ in isotype, $n = 10$/other groups). On days 8, 11, 15, and 18, treated mice received intratumoral injections of immunoswitch or isotype particles, and tumors were measured every 2–3 days.

Immunoswitch Biodistribution.

Immunoswitch particles were synthesized as described above. Immunoswitch particles and a mixture of soluble anti-4-1BB and anti-PD-L1 antibody were labeled with IRDye 680RD protein labeled kits from LI-COR Biosciences (Lincoln, Nebraska, USA) according to the manufacturer's protocol.

Nu/J mice (Jackson Laboratories, Bar Harbor, ME, USA) were injected with equal protein amounts of either IR-labeled soluble antibody or immunoswitch particles subcutaneously on the right flank ($n = 3$/group). Dorsal, ventral, right, and left images of the mice were taken at 3, 24, 48, and 72 h post-injection. Only the right images which show the injection area are shown. All images from any individual mouse had matched thresholding. Images were analyzed in ImageJ by defining a region of interest (ROI) around the initial injection site which was then duplicated in all images. The mean gray value of each ROI was then measured in ImageJ. The mean gray value for an image of an individual mouse at time T was then normalized to the mean gray value at 3 h using the following equation:

$$\text{mean gray value (normalized)} = \frac{\text{mean gray value}_{t=T}}{\text{mean gray value}_{t=3}}$$

These data were then fit to a one-phase exponential decay curve using the GraphPad nonlinear regression analysis module (GraphPad Software, La Jolla, CA, USA).

For organ analysis studies, C57BL/6 mice ($n = 3$/group) were injected subcutaneously with B16-SIY cells on day 0. Eight days later, IR-labeled immunoswitch particles were injected intratumorally into half of the tumor-bearing mice. 48 h after treatment, the tumor, spleen, tumor-draining lymph node, and contralateral lymph node of each mouse were dissected and imaged on an IR imager. Images were analyzed in ImageJ by defining a ROI around each lymph node which was then duplicated in all images. Tumor and spleen ROI were defined for each image independently due to their difference in size and shape. The mean gray value of each ROI was then measured in ImageJ and was normalized to the maximum of the sensor.

Conjugation Assay.

2C CD8+ T cells were isolated from naïve splenoctyes and stimulated on days −8 and −4 with expander beads as previously described. B16-F10 cells were incubated with media supplemented with 20 ng/mL recombinant murine IFN-γ (R&D Systems, Minneapolis, MN, USA) on day −2 for 48 h.

On day 0, CD8 cells and B16-F10 cells were isolated from beads and IFN-γ, respectively, as previously described. CD8 cell membranes were labeled with the PKH26 red fluorescent

cell linker kit, and B16-F10 cell membranes were labeled with the PKH67 green fluorescent cell linker kit (Sigma-Aldrich, St. Louis, MO, USA) according to the manufacturer's protocol. Effector and target cells were co-incubated at a 1:1 ratio with immunoswitch or isotype particles. After 1 h, cells were briefly vortexed and fixed. For flow cytometry experiments, cells were fixed in 0.5% paraformaldehyde for 20 min at room temperature. Cells were then read on a BD FacsCalibur. Conjugate formation was measured by first gating on all CD8+ T cells (*i.e.*, red cells) and then on those also bound to B16-F10 cells (*i.e.*, also expressing green) using FlowJo (TreeStar). Flow cytometry experiments were repeated three independent times. For confocal microscopy experiments, cells were fixed in 2% paraformaldehyde for 20 min at room temperature. Cells were then read on a Zeiss LSM510-Meta laser scanning confocal microscope at 100× magnification. Two to three nonoverlapping images were taken per experiment, and the experiment was repeated three independent times. Conjugate formation was determined manually by observing red/green overlap/contact using ImageJ. Each image was taken as an independent data point. For both flow cytometry and confocal microscopy studies, conjugation was measured as the percent of CD8 cells forming conjugates with B16-F10 cells divided by the total number of CD8 cells.

Statistics.

Information on statistical tests is present in all figure legends. One and two-way ANOVA were used when making multiple comparisons. Bonferroni post-tests were performed when comparing all groups, and Dunnett's post-tests were performed when the hypotheses being tested involved comparison against a single group. One-tailed and two-tailed *t* tests were used when comparing two groups, as indicated in figure legends. All data sets were assumed to fit a normal distribution, and all graphs show mean and error bars represent SEM. All *n* values are present within figure legends. *In vivo* tumor treatment studies were repeated in two independent experiments to ensure adequate sample size and reproducibility. Mice with outlier tumor size before the beginning of treatment were removed from the studies. Randomization was performed by cage in all animal studies. All statistical analysis was performed using GraphPad Prism software.

Supplementary Material

Refer to Web version on PubMed Central for supplementary material.

ACKNOWLEDGMENTS

A.K.K. thanks the National Science Foundation (DGE-1232825), the NIH Cancer Nanotechnology Training Center at the JHU Institute for Nanobiotechnology (2T32CA153952-06), and the National Cancer Institute of the NIH (F31CA206344) for fellowship support. We also acknowledge support from the National Institutes of Health (P01-AI072677, R01-CA108835, R21-CA185819), TEDCO/Maryland Innovation Initiative and the Coulter Foundation (J.P.S.). We thank Qiongman Kong for technical support.

REFERENCES

(1). Chen DS; Mellman I Oncology Meets Immunology: The Cancer-Immunity Cycle. Immunity 2013, 39, 1–10. [PubMed: 23890059]

(2). Schreiber RD; Old LJ; Smyth MJ Cancer Immunoediting: Integrating Immunity's Roles in Cancer Suppression and Promotion. Science 2011, 331, 1565–1570. [PubMed: 21436444]

(3). Rosenberg SA; Restifo NP Adoptive Cell Transfer as Personalized Immunotherapy for Human Cancer. Science 2015, 348, 62–68. [PubMed: 25838374]

(4). Oelke M; Schneck JP Overview of a HLA-Ig based "Lego-like System" for T Cell Monitoring, Modulation and Expansion. Immunol. Res 2010, 47, 248–256. [PubMed: 20087680]

(5). Barrett DM; Singh N; Porter DL; Grupp SA; June CH Chimeric Antigen Receptor Therapy for Cancer. Annu. Rev. Med 2014, 65, 333–347. [PubMed: 24274181]

(6). Peggs KS; Quezada SA PD-1 Blockade: Promoting Endogenous Anti-Tumor Immunity. Expert Rev. Anticancer Ther 2012, 12, 1279–1282. [PubMed: 23176616]

(7). June CH; Riddell SR; Schumacher TN Adoptive Cellular Therapy: A Race to the Finish Line. Sci. Transl. Med 2015, 7, 280ps7.

(8). Chen L; Flies DB Molecular Mechanisms of T Cell Co-Stimulation and Co-Inhibition. Nat. Rev. Immunol 2013, 13, 227–242. [PubMed: 23470321]

(9). Zhang H; Snyder KM; Suhoski MM; Maus MV; Kapoor V; June CH; Mackall CL 4-1BB Is Superior to CD28 Costimulation for Generating CD8+ Cytotoxic Lymphocytes for Adoptive Immunotherapy. J. Immunol 2007, 179, 4910–4918. [PubMed: 17878391]

(10). Shuford WW; Klussman K; Tritchler DD; Loo DT; Chalupny J; Siadak AW; Brown TJ; Emswiler J; Raecho H; Larsen CP; Pearson TC; Ledbetter JA; Aruffo A; Mittler RS 4-1BB Costimulatory Signals Preferentially Induce CD8+ T Cell Proliferation and Lead to the Amplification *in Vivo* of Cytotoxic T Cell Responses. J. Exp. Med 1997, 186, 47–55. [PubMed: 9206996]

(11). Oh HS; Choi BK; Kim YH; Lee DG; Hwang S; Lee MJ; Park SH; Bae Y-S; Kwon BS 4-1BB Signaling Enhances Primary and Secondary Population Expansion of CD8+ T Cells by Maximizing Autocrine IL-2/IL-2 Receptor Signaling. PLoS One 2015, 10, e0126765. [PubMed: 25962156]

(12). Freeman GJ; Sharpe AH; Kuchroo VK Protect the Killer: CTLs Need Defenses against the Tumor. Nat. Med 2002, 8, 787–789. [PubMed: 12152031]

(13). Ahmad M; Rees RC; Ali SA Escape from Immunotherapy: Possible Mechanisms That Influence Tumor Regression/progression. Cancer Immunol. Immunother 2004, 53, 844–854. [PubMed: 15197495]

(14). Bono MR; Fernández D; Flores-Santibáñez F; Rosemblatt M; Sauma D CD73 and CD39 Ectonucleotidases in T Cell Differentiation: Beyond Immunosuppression. FEBS Lett. 2015, 589, 3454–3460. [PubMed: 26226423]

(15). Rabinovich GA; Gabrilovich D; Sotomayor EM Immunosuppressive Strategies That Are Mediated by Tumor Cells. Annu. Rev. Immunol 2007, 25, 267–296. [PubMed: 17134371]

(16). Vasievich EA; Huang L The Suppressive Tumor Microenvironment: A Challenge in Cancer Immunotherapy. Mol. Pharmaceutics 2011, 8, 635–641.

(17). Zhou Q; Xiao H; Liu Y; Peng Y; Hong Y; Yagita H; Chandler P; Munn DH; Mellor A; Fu N; He Y Blockade of Programmed Death-1 Pathway Rescues the Effector Function of Tumor-Infiltrating T Cells and Enhances the Antitumor Efficacy of Lentivector Immunization. J. Immunol 2010, 185, 5082–5092. [PubMed: 20926790]

(18). Kamphorst AO; Ahmed R Manipulating the PD-1 Pathway to Improve Immunity. Curr. Opin. Immunol 2013, 25, 381–388. [PubMed: 23582509]

(19). Iwai Y; Ishida M; Tanaka Y; Okazaki T; Honjo T; Minato N Involvement of PD-L1 on Tumor Cells in the Escape from Host Immune System and Tumor Immunotherapy by PD-L1 Blockade. Proc. Natl. Acad. Sci. U. S. A 2002, 99, 12293–12297. [PubMed: 12218188]

(20). Karwacz K; Bricogne C; MacDonald D; Arce F; Bennett CL; Collins M; Escors D PD-L1 Co-Stimulation Contributes to Ligand-Induced T Cell Receptor down-Modulation on CD8+ T Cells. EMBO Mol. Med 2011, 3, 581–592. [PubMed: 21739608]

(21). Pilon-Thomas S; Mackay A; Vohra N; Mulé JJ Blockade of Programmed Death Ligand 1 Enhances the Therapeutic Efficacy of Combination Immunotherapy against Melanoma. J. Immunol 2010, 184, 3442–3449. [PubMed: 20194714]

(22). Callahan MK; Wolchok JD At the Bedside: CTLA-4- and PD-1-Blocking Antibodies in Cancer Immunotherapy. J. Leukocyte Biol 2013, 94, 41–53. [PubMed: 23667165]

(23). Ascierto PA; Marincola FM 2015: The Year of Anti-PD-1/PD-L1s Against Melanoma and Beyond. EBioMedicine 2015, 2, 92–93. [PubMed: 26137543]

(24). Robert C; Long GV; Brady B; Dutriaux C; Maio M; Mortier L; Hassel JC; Rutkowski P; McNeil C; Kalinka-Warzocha E; Savage KJ; Hernberg MM; Lebbé C; Charles J; Mihalcioiu C; Chiarion-Sileni V; Mauch C; Cognetti F; Arance A; Schmidt H; et al. Nivolumab in Previously Untreated Melanoma without BRAF Mutation. N. Engl. J. Med 2015, 372, 320–330. [PubMed: 25399552]

(25). Robert C; Ribas A; Wolchok JD; Hodi FS; Hamid O; Kefford R; Weber JS; Joshua AM; Hwu W-J; Gangadhar TC; Patnaik A; Dronca R; Zarour H; Joseph RW; Boasberg P; Chmielowski B; Mateus C; Postow M. a; Gergich K; Elassaiss-Schaap J; et al. Anti-Programmed-Death-Receptor-1 Treatment with Pembrolizumab in Ipilimumab-Refractory Advanced Melanoma: A Randomised Dose-Comparison Cohort of a Phase 1 Trial. Lancet 2014, 384, 1109–1117. [PubMed: 25034862]

(26). Topalian SL; Hodi FS; Brahmer JR; Gettinger SN; Smith DC; McDermott DF; Powderly JD; Carvajal RD; Sosman JA; Atkins MB; Leming PD; Spigel DR; Antonia SJ; Horn L; Drake CG; Pardoll DM; Chen L; Sharfman WH; Anders RA; Taube JM; et al. Safety, Activity, and Immune Correlates of Anti-PD-1 Antibody in Cancer. N. Engl. J. Med 2012, 366, 2443–2454. [PubMed: 22658127]

(27). Brahmer JR; Tykodi SS; Chow LQ; Hwu WJ; Topalian SL; Hwu P; Drake CG; Camacho LH; Kauh J; Odunsi K; Pitot HC; Hamid O; Bhatia S; Martins R; Eaton K; Chen S; Salay TM; Alaparthy S; Grosso JF; Korman AJ; et al. Safety and Activity of Anti-PD-L1 Antibody in Patients with Advanced Cancer. N. Engl. J. Med 2012, 366, 2455–2465. [PubMed: 22658128]

(28). Larkin J; Chiarion-Sileni V; Gonzalez R; Grob JJ; Cowey CL; Lao CD; Schadendorf D; Dummer R; Smylie M; Rutkowski P; Ferrucci PF; Hill A; Wagstaff J; Carlino MS; Haanen JB; Maio M; Marquez-Rodas I; McArthur GA; Ascierto PA; Long GV; et al. Combined Nivolumab and Ipilimumab or Monotherapy in Untreated Melanoma. N. Engl. J. Med 2015, 373, 23–34. [PubMed: 26027431]

(29). Spranger S; Koblish HK; Horton B; Scherle PA; Newton R; Gajewski TF Mechanism of Tumor Rejection with Doublets of CTLA-4, PD-1/PD-L1, or IDO Blockade Involves Restored IL-2 Production and Proliferation of CD8(+) T Cells Directly within the Tumor Microenvironment. J. Immunother. cancer 2014, 2, 3. [PubMed: 24829760]

(30). Chen S; Lee L-F; Fisher TS; Jessen B; Elliott M; Evering W; Logronio K; Tu GH; Tsaparikos K; Li X; Wang H; Ying C; Xiong M; VanArsdale T; Lin JC Combination of 4-1BB Agonist and PD-1 Antagonist Promotes Antitumor Effector/Memory CD8 T Cells in a Poorly Immunogenic Tumor Model. Cancer Immunol. Res 2015, 3, 149–160. [PubMed: 25387892]

(31). Blank C; Brown I; Peterson AC; Spiotto M; Iwai Y; Honjo T; Gajewski TF PD-L1/B7H-1 Inhibits the Effector Phase of Tumor Rejection by T Cell Receptor (TCR) Transgenic CD8 + T Cells PD-L1/B7H-1 Inhibits the Effector Phase of Tumor Rejection by T Cell Receptor. Cancer Res. 2004, 64, 1140–1145. [PubMed: 14871849]

(32). Vezys V; Penaloza-MacMaster P; Barber DL; Ha S; Konieczny B; Freeman GJ; Mittler RS; Ahmed R 4-1BB Signaling Synergizes with Programmed Death Ligand 1 Blockade To Augment CD8 T Cell Responses during Chronic Viral Infection. J. Immunol 2011, 187, 1634–1642. [PubMed: 21742975]

(33). Perica K; Bieler JG; Schutz C; Varela JC; Douglass J; Skora A; Chiu YL; Oelke M; Kinzler K; Zhou S; Vogelstein B; Schneck JP Enrichment and Expansion with Nanoscale Artificial Antigen Presenting Cells for Adoptive Immunotherapy. ACS Nano 2015, 9, 6861–6871. [PubMed: 26171764]

(34). Kwong B; Gai SA; Elkhader J; Wittrup KD; Irvine DJ Localized Immunotherapy *via* Liposome-Anchored Anti-CD137 + IL-2 Prevents Lethal Toxicity and Elicits Local and Systemic Antitumor Immunity. Cancer Res. 2013, 73, 1547–1558. [PubMed: 23436794]

(35). Kwong B; Liu H; Irvine DJ Induction of Potent Anti-Tumor Responses While Eliminating Systemic Side Effects *via* Liposome-Anchored Combinatorial Immunotherapy. Biomaterials 2011, 32, 5134–5147. [PubMed: 21514665]

(36). Khong HT; Restifo NP Natural Selection of Tumor Variants in the Generation of “Tumor Escape” Phenotypes. Nat. Immunol 2002, 3, 999–1005. [PubMed: 12407407]

(37). Snyder A; Makarov V; Merghoub T; Yuan J; Zaretsky JM; Desrichard A; Walsh LA; Postow MA; Wong P; Ho TS; Hollmann TJ; Bruggeman C; Kannan K; Li Y; Elipenahli C; Liu C; Harbison CT; Wang L; Ribas A; Wolchok JD; Chan TA Genetic Basis for Clinical Response to CTLA-4 Blockade in Melanoma. N. Engl. J. Med 2014, 371, 2189–2199. [PubMed: 25409260]

(38). Carreno BM; Magrini V; Becker-Hapak M; Kaabinejadian S; Hundal J; Petti AA; Ly A; Lie W; Hildebrand WH; Mardis ER; Linette GP A Dendritic Cell Vaccine Increases the Breadth and Diversity of Melanoma Neoantigen-Specific T Cells. Science 2015, 348, 803–808. [PubMed: 25837513]

(39). Manolova V; Flace A; Bauer M; Schwarz K; Saudan P; Bachmann MF Nanoparticles Target Distinct Dendritic Cell Populations according to Their Size. Eur. J. Immunol 2008, 38, 1404–1413. [PubMed: 18389478]

(40). Toy R; Peiris PM; Ghaghada KB; Karathanasis E Shaping Cancer Nanomedicine: The Effect of Particle Shape on the *in Vivo* Journey of Nanoparticles. Nanomedicine (London, U. K.) 2014, 9, 121–134.

(41). Steenblock ER; Fadel T; Labowsky M; Pober JS; Fahmy TM An Artificial Antigen-Presenting Cell with Paracrine Delivery of IL-2 Impacts the Magnitude and Direction of the T Cell Response. J. Biol. Chem 2011, 286, 34883–34892. [PubMed: 21849500]

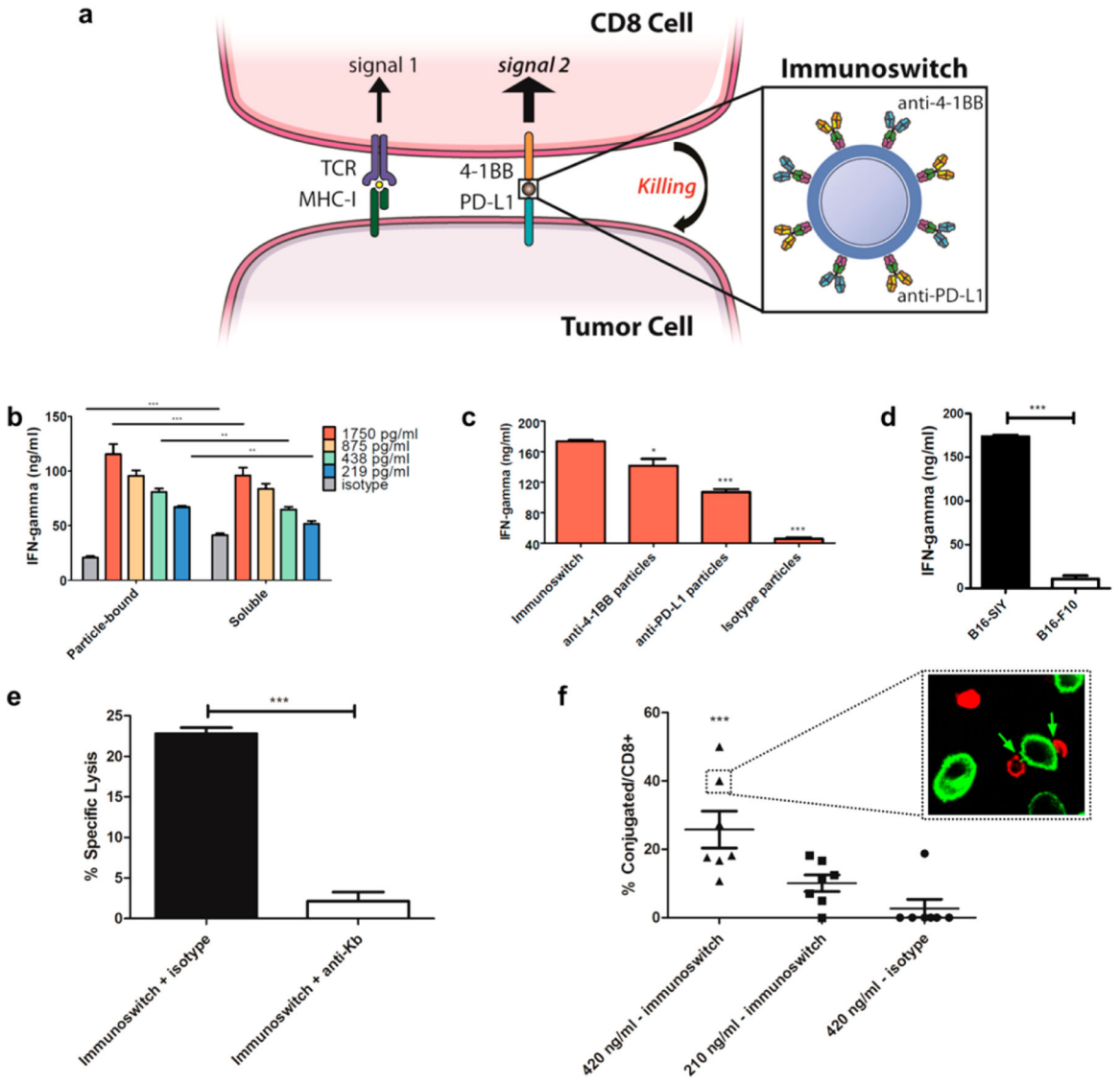

Figure 1.

Immunoswitch particles link PD-L1 checkpoint blockade with 4-1BB co-stimulation. (a) Schematic showing immunoswitch particle interaction with CD8+ T cell and cognate target cell. Inset: Immunoswitch particles are synthesized by conjugating anti-4-1BB and anti-PD-L1 monoclonal antibodies to the surface of 80 nm particles. (b) IFN-γ secretion from PD-1^{hi} 2C CD8 cells co-incubated with PD-L1^{hi} cognate B16-SIY cells and immunoswitch particles or soluble antibody. Concentrations refer to total antibody in culture. Significance measured by two-way ANOVA with Bonferroni post-test ($p = 0.0064$, $F_{1,30} = 8.607$ treatment variation; $p < 0.0001$, $F_{4,30} = 79.76$ concentration variation). (c) IFN-γ secretion from PD-1^{hi} CD8 cells co-incubated with PD-L1^{hi} B16-SIY and 9 μg/mL of the indicated particle type. Significance measured by one-way ANOVA with Dunnett's post-test. Comparisons to immunoswitch particles are shown. (d) IFN-γ secretion from PD-1^{hi} 2C CD8 cells co-incubated with PD-L1^{hi} cognate B16-SIY cells or noncognate B16-F10 cells and immunoswitch particles. Significance was measured by two-tailed t test

($p < 0.0001$). Mean ± SEM of three samples is shown for (b–d). (e) Percent specific lysis of B16-SIY cells by 2C CD8+ T cells when co-incubated for 4 h at a 1:1 effector-target ratio in the presence of immunoswitch particles and 100 μg/mL anti-Kb blocking mAb or isotype control. Significance was measured by two-tailed *t* test. (f) PD-1^{hi} 2C CD8 cells and PD-$L1^{hi}$ B16-F10 cells were labeled with a red and green membrane dye, respectively. Percent of CD8 cells forming conjugates were counted. Each data point represents an independent image taken across three independent experiments. 420 ng/ml of immunoswitch particles significantly increased conjugation rate over isotype particles as measured by one-way ANOVA ($p = 0.0013$) with Dunnett's post-test. Arrows show conjugate formation. ***$p < 0.001$, **$p < 0.01$, *$p < 0.05$. Cell and antibody images in (a) are adapted under a Creative Commons License from Servier Medical Art (http://www.servier.com/Powerpoint-image-bank).

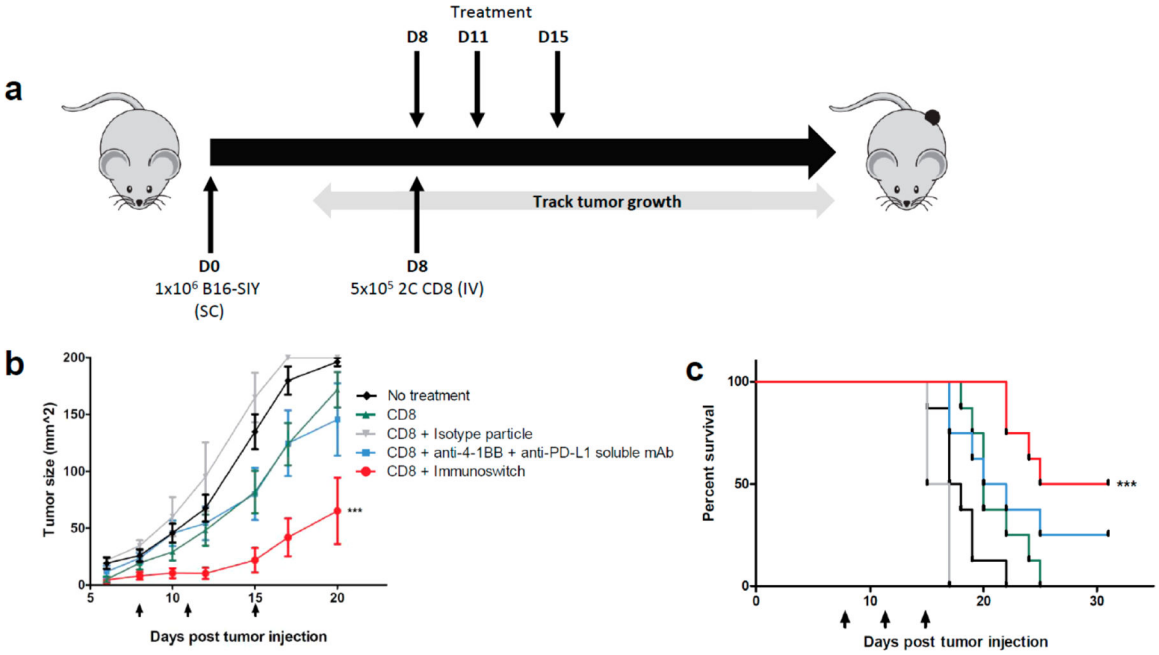

Figure 2.

Immunoswitch particles inhibits tumor growth *in vivo*. (a) Schematic showing our *in vivo* model. C57BL/6 mice ($n = 4$ isotype, $n = 8$ all other groups) were injected with 1×10^6 B16-SIY cells subcutaneously (SC) on day 0. 2C CD8 cells were isolated on day 0, stimulated with anti-CD3/anti-CD28 expander beads on days 0 and 4 as previously described,[25] and isolated from the beads and injected intravenously (IV) on day 8. Particle and antibody treatments were given intratumorally (IT) on days 8, 11, and 15. (b) Tumor growth curves show only immunoswitch treatment significantly delayed tumor growth as compared to no treatment and all other controls, past day 15. Black arrows indicate treatment days. Significance measured by two-way ANOVA with Bonferroni post-test ($p < 0.001$). (c) Immunoswitch treatment significantly extended survival as compared to no treatment. Significance measured by log-rank test ($p = 0.0002$). Combined results from two independent experiments are shown. ***$p < 0.001$.

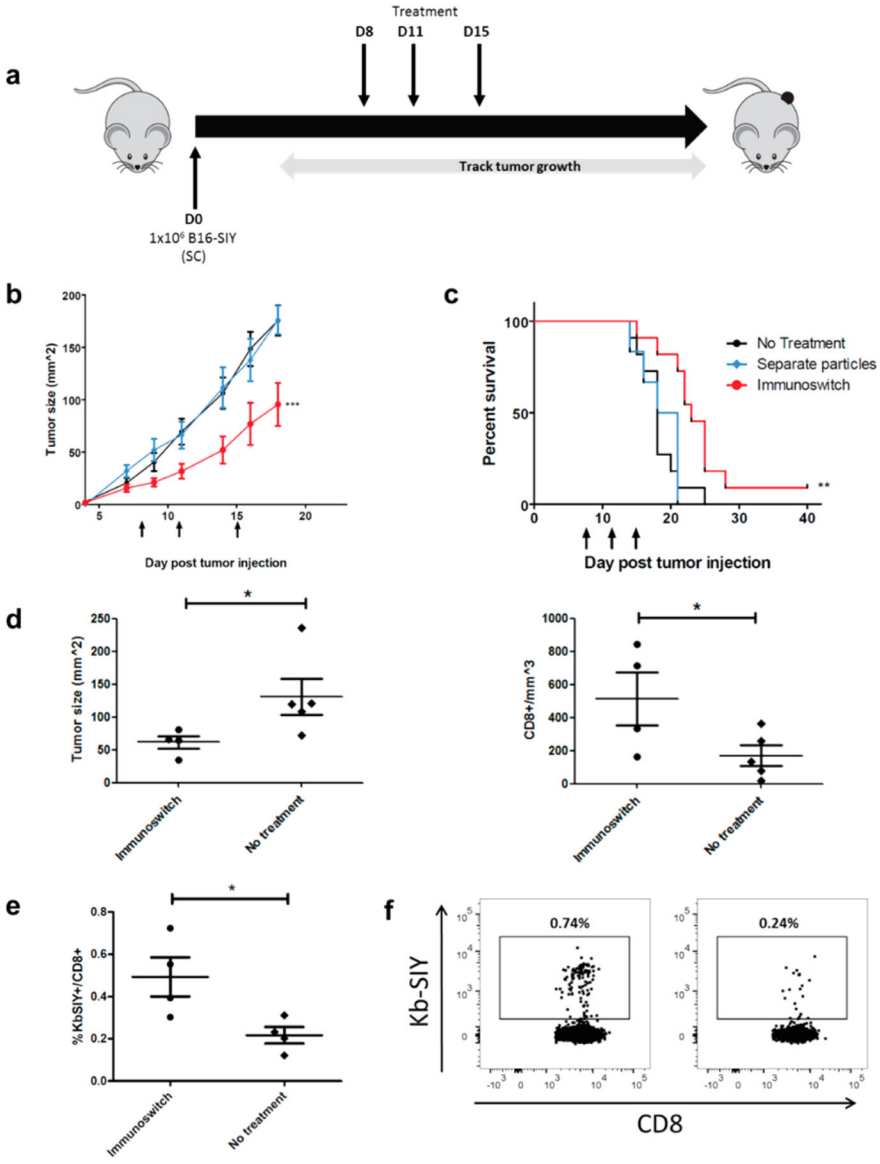

Figure 3.

Immunoswitch particles delay tumor growth in the absence of adoptively transferred cells. (a) C57BL/6 mice (n = 6 separate particle treatment, n = 11/other groups) were injected with B16-SIY cells SC on day 0. Treatment with either immunoswitch particles or a co-injection of anti-4-1BB and anti-PD-L1 particles was injected IT on days 8, 11, and 15. No adoptive transfer of tumor-specific cells was given. (b) Immunoswitch particles, but not separate anti-4-1BB and anti-PD-L1 mAb particles, delayed tumor growth compared to no treatment at all time points past day 11. Arrows indicate treatment days. Significance was measured by two-way ANOVA with Bonferroni post-test (p = 0.007). (c) Only immunoswitch particle treatment significantly extended survival. Significance was measured by log-rank test (p = 0.0066). Results from two independent experiments are combined for (a–c). (d) C57BL/6 mice (n = 5/group) were injected with B16-SIY cells as above, and half were treated with immunoswitch particles IT on days 8 and 11. On day 14, tumor-infiltrating lymphocytes

and tumor-draining lymph nodes were harvested and analyzed. The nontreated group had significantly larger tumors ($p = 0.034$) and a lower CD8+ T cell density ($p = 0.032$) within the tumor on day 14. Significance was measured by two-tailed *t* test. (e) CD8+ cells within the tumor-draining lymph nodes of immunoswitch-treated mice had higher Kb-SIY (expressed by tumor) specificity. Significance was measured by two-tailed *t* test ($p = 0.033$). (f) Representative flow plots showing Kb-SIY specificity of CD8+ T cells from tumor-draining lymph nodes of immunoswitch (left) or nontreated (right) mice. ***$p < 0.001$, **$p < 0.01$, *$p < 0.05$.

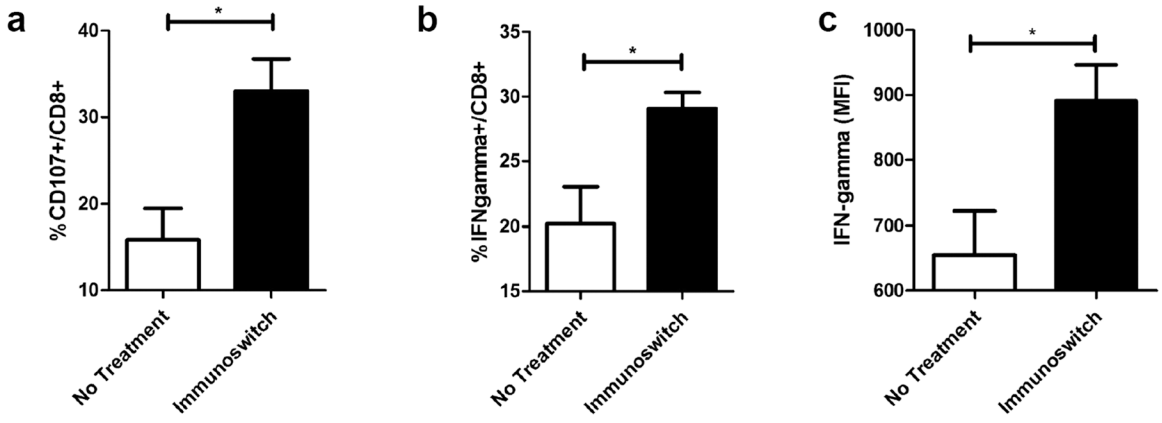

Figure 4.

Tumor-specific CD8+ tumor-infiltrating lymphocytes of immunoswitch treated mice have increased functionality. (a) C57BL/6 mice (n = 3/group) were injected with B16-SIY cells SC on day 0. Immunoswitch particles were injected IT on days 8 and 11. On day 14, tumor-infiltrating lymphocytes were harvested and restimulated with SIY pulsed RMA-S cells. Intracellular cytokine staining indicated an increased frequency of CD107 producing (a) and IFN-γ producing (b) CD8+ T cells following immunoswitch treatment. The mean fluorescence intensity (MFI) of IFN-γ+ cells was increased in treated mice. Significance was measured by one-tailed t test (*$p < 0.05$).

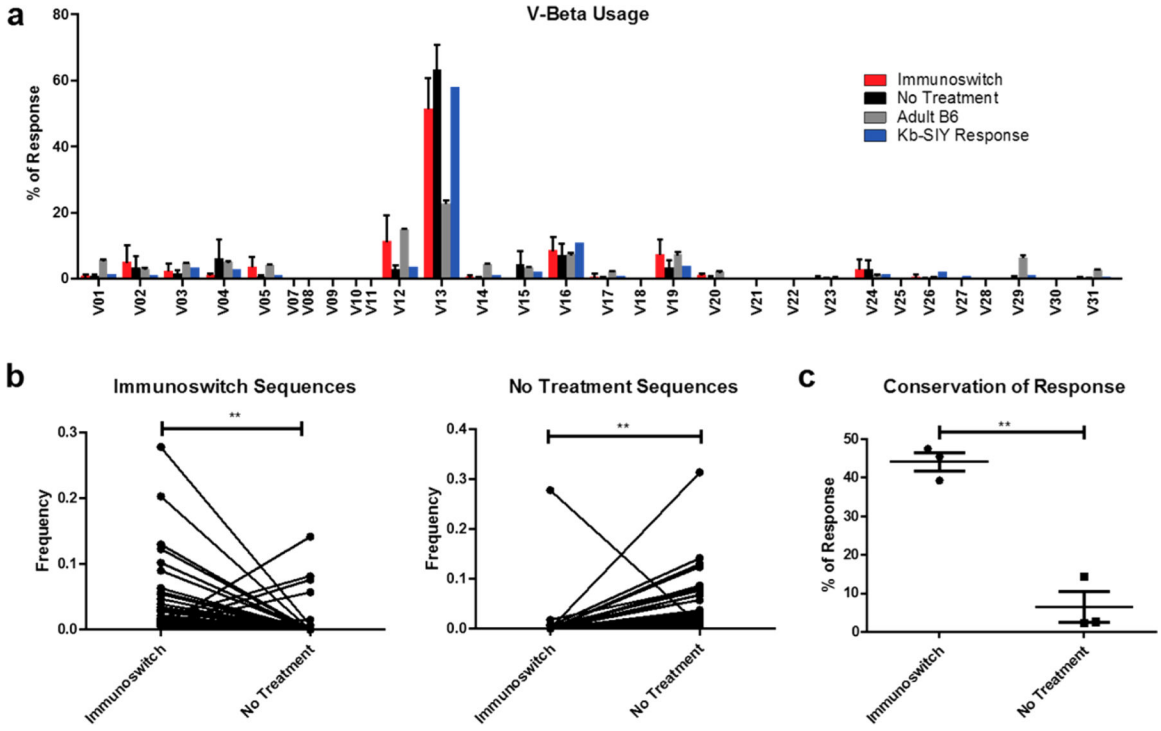

Figure 5.

Immunoswitch treatment alters the CD8+ T cell repertoire. (a) T cell receptor V-beta usage in CD8+ tumor-infiltrating lymphocytes from immunoswitch-treated, nontreated, nontumor bearing adult B6 mice, or a Kb-SIY-specific CD8+ T cell response. C57BL/6 mice (n = 3/group) were injected with B16-SIY cells SC on day 0. Immunoswitch particles were injected IT into treated mice on days 8 and 11, and tumor-infiltrating lymphocytes were isolated on day 14. Immunoswitch treated and nontreated mice skew toward T cell receptor V-beta 13, as is seen in a Kb-SIY specific response. (b) T cell receptor clones present in the CD8+ tumor-infiltrating lymphocytes of immunoswitch-treated mice are present at significantly higher frequencies than in the tumor-infiltrating lymphocytes of nontreated mice (left). T cell receptor clones present in the CD8+ tumor-infiltrating lymphocytes of nontreated mice are present at significantly higher frequencies than in the tumor-infiltrating lymphocytes of immunoswitch-treated mice (right). Significance measured by two-tailed paired t test ($p < 0.01$). (c) CD8+ T cell receptor clones are conserved to a significantly higher extent in immunoswitch-treated mice. Each point represents the percent of overlapping clonal response between two mice of the same group. Significance measured by two-tailed t test ($p < 0.01$).

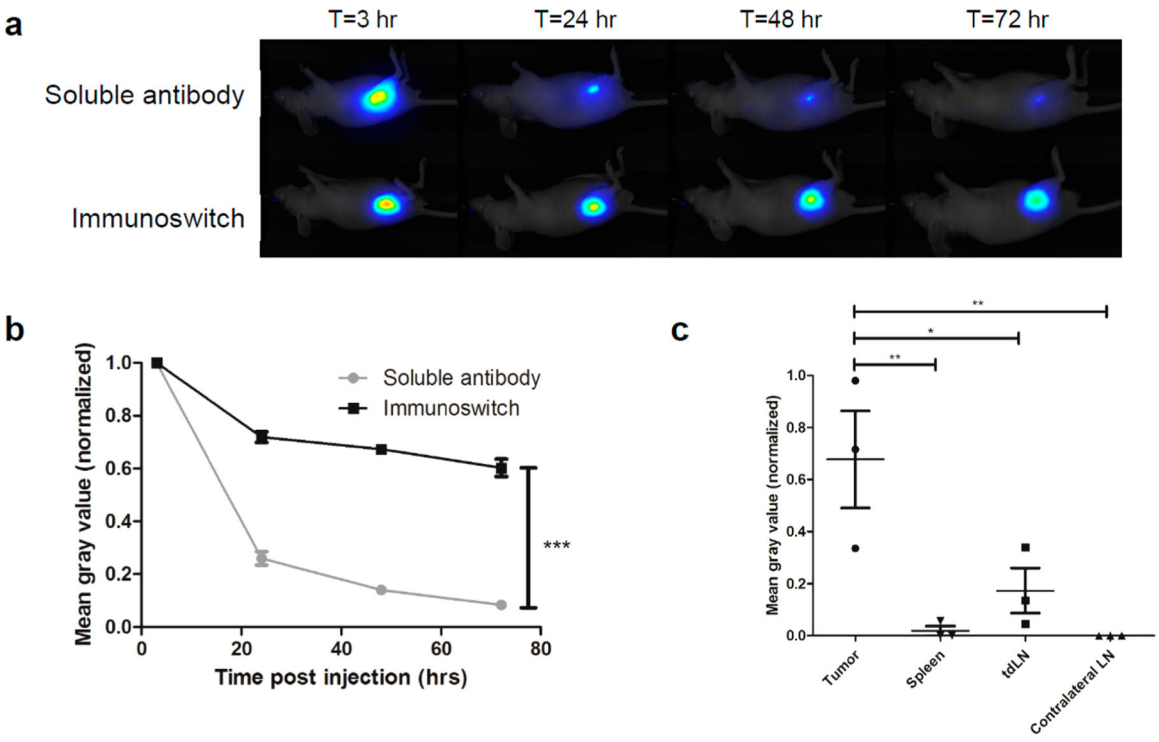

Figure 6.

Immunoswitch particles remain at the injection site longer than soluble antibody. (a) Nude mice (n = 3/group) were injected with IR-labeled soluble antibody or immunoswitch particles at t = 0 h. Mice were imaged with a full body IR imager at t = 3, 24, 48, and 72 h post-injection. (b) Change in the mean gray value over time in the target ROI. Images from individual mice were normalized to the mean gray value at t = 3 h (see Methods section). An immediate decrease is observed after injection, followed by a consistent clearance rate. Clearance from the injection site is greater for soluble antibodies than immunoswitch particles at all time points: $t_{1/2,\text{soluble}}$ = 15.2 h and $t_{1/2,\text{immunoswitch}}$ = 84.5 h when fit to a one phase decay equation. Significance measured by two-way ANOVA with Bonferroni post-test ($p < 0.0001$, $F_{1,16} = 995.7$ treatment variation). (c) C57BL/6 mice (n = 3) were injected with IR-labeled immunoswitch particles 8 days after B16-SIY inoculation. Tumor, spleen, tumor-draining lymph node, and contralateral lymph node were harvested 48 h after treatment. Immunoswitch particles are retained primarily in the tumor and tumor-draining lymph node. Values were recorded relative to the sensor's maximum (*i.e.*, 0–1 scale). Significance measured by two-way ANOVA with Tukey's post-test (*$p < 0.05$, **$p < 0.01$,***$p < 0.001$).

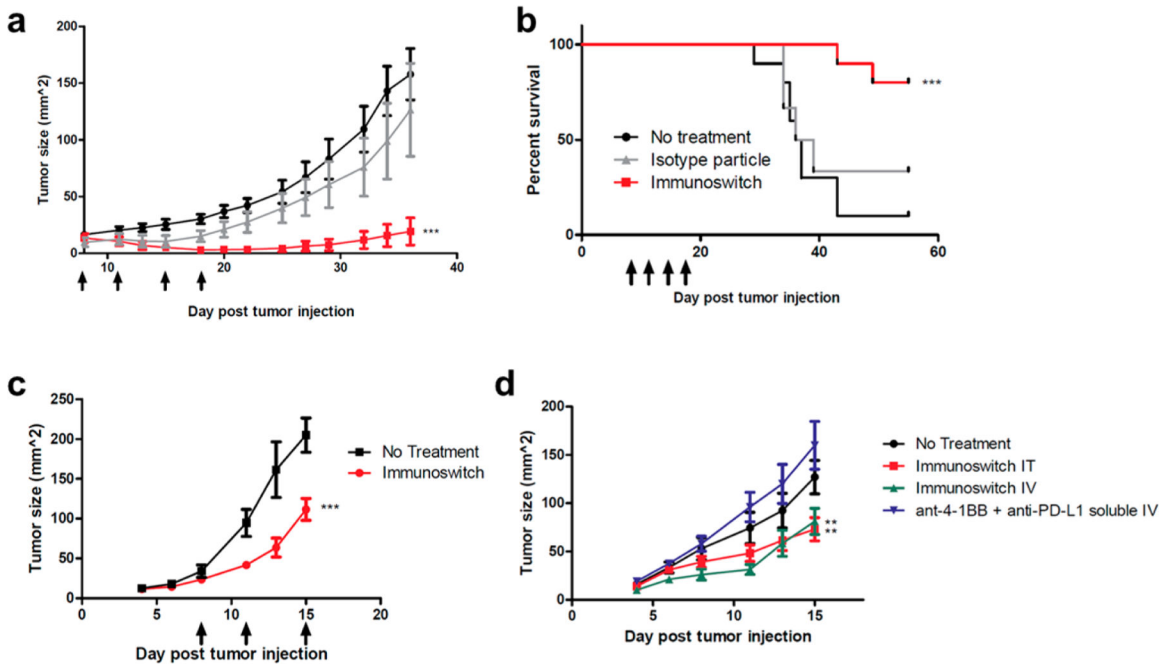

Figure 7.

Immunoswitch particles reverse tumor growth and extend survival in multiple tumor models and injection routes. (a) C57BL/6 mice ($n = 6$ in isotype, $n = 10$/other groups) were injected with MC38-OVA murine colon cancer cells SC on day 0. Treated mice received IT injections on days 8, 11, 15, and 18. Only immunoswitch particles significantly delayed and reversed tumor growth as compared with no treatment, past day 22. Significance was measured by two-way ANOVA with Bonferroni post-test ($p = 0.0003$). Arrows indicate treatment days. (b) Only immunoswitch particles significantly extended survival as compared to no treatment, as measured by log-rank test. Combined results from two independent experiments are shown. (c) C57BL/6 mice ($n = 5$/group) were injected with B16-F10 cells SC on day 0. Treated mice received IT injections on days 8, 11, and 15. Immunoswitch treatment delayed tumor growth as compared to no treatment, past day 11. Significance was measured by two-way ANOVA with Bonferroni post-test. Arrows indicate treatment days. (d) C57BL/6 mice ($n \geq 5$/group) were injected with B16-SIY cells SC on day 0. IV immunoswitch particles were administered on days 4, 8, 11, and 15 and days 8, 11, and 15 by IT. Immunoswitch particles injected either IT or IV delay tumor growth past day 13 compared to no treatment ($p < 0.01$). Soluble injected antibody has no effect on tumor growth. Significance was measured by two-way ANOVA with Bonferroni post-test (**$p < 0.01$, ***$p < 0.001$).